Faculty Publications   Chemical Engineering, Department of

Studies on the Capacitance of Nickel Oxide Films: Effect of Heating Temperature and Electrolyte Concentration

Venkat Srinivasan
University of South Carolina - Columbia

John W. Weidner
University of South Carolina - Columbia, weidner@engr.sc.edu

Studies on the Capacitance of Nickel Oxide Films: Effect of Heating Temperature and Electrolyte Concentration

Venkat Srinivasan* and John W. Weidner**,z

Department of Chemical Engineering, University of South Carolina, Columbia, South Carolina 29208, USA

Nickel oxide films were prepared by electrochemically precipitating the hydroxide and heating it in air to form the oxide. The resulting oxide films behave as a capacitor. The capacitance of the oxide depends on the heating temperature, showing a maximum at 300°C. The mechanism of charge storage was studied by measuring the capacitance and surface area as a function of heating temperature, and the capacitance in different electrolytes and potential windows. The charge-storage mechanism is believed to be a surface redox reaction involving adsorbed hydroxyl ions.

© 2000 The Electrochemical Society. S0013-4651(99)07-034-2. All rights reserved.

With the increasing interest in high-power devices (*e.g.*, for acceleration in electric vehicles), electrochemical capacitors (ECs) have been studied extensively in recent years (see, for example, Ref. 1-3). Most commercially available ECs make use of the double layer formed at the electrode/electrolyte interface to store energy. As the double-layer capacitance is typically less than 40 $\mu F/cm^2$, [4] high-surface-area materials such as activated carbon are usually used. However, as much as 90% of the available surface area is not utilized in activated carbon due to the presence of micropores (<2 nm), which cannot be wetted by the electrolyte.[5] Another strategy for increasing the energy stored in these devices is the use of faradaic pseudocapacitors, which exhibit current-potential responses similar to that of double-layer capacitors. Transition metal oxides like RuO_2[6,7] and IrO_2[7] exhibit faradaic pseudocapacitance with capacitance reported to be as large as 760 F/g.[6] (Note that all capacitance values reported in this paper are for a single electrode excluding the mass of the separator, electrolyte, and current collectors.) However, the high cost of ruthenium and iridium has stimulated research for identifying other materials that exhibit similar behavior.

Recently Liu and Anderson[8-11] reported the pseudocapacitance of nickel oxide (*i.e.*, NiO) films that were made by heating sol-gel-derived nickel hydroxide [*i.e.*, $Ni(OH)_2$] in air at 300°C. We investigated similar nickel oxide films, the only difference being that the nickel hydroxide was produced via electrochemical deposition.[12] Both groups reported a specific capacitance as high as 260 F/g. The films also maintain high utilization at high power densities and have excellent cycle life.[12] Even though the specific capacitance is comparable to that of activated carbon,[5] the ability to make thin films makes NiO attractive for high-power devices.

What is not known though is how heating temperature, electrolyte environment, or the potential range of operation affect the capacitance of nickel oxide. Therefore, in order to understand the mechanism of charge storage in these materials, the specific (*i.e.*, capacitance per mass of material) and intrinsic (*i.e.*, capacitance per surface area) capacitance are reported as a function of heating temperature (25-450°C), electrolyte environment (3-40 wt % KOH, and 1 N H_2SO_4), and potential window of operation (−0.55 to 0.45 V *vs.* SCE). This insight can be used to guide electrode development, which may enable NiO to be a commercially viable electrode in ECs.

Experimental

Thin films of nickel hydroxide were deposited on gold foils masked with a sealant (Silicone™) so as to expose an area of 1.0 cm^2. The films studied here were deposited at room temperature in a bath containing 1.8 M $Ni(NO_3)_2$ and 0.075 M $NaNO_3$ in a solvent of 50 vol % ethanol in a procedure described in detail elsewhere.[13,14] A cathodic current density of 5.0 mA/cm^2 was applied for

25 min, which according to these previous deposition studies should result in 350 μg films with a capacity of 277 mC (*i.e.*, 790 C/g). The expected capacity was confirmed by performing cyclic voltammetry on nickel hydroxide in 3 wt % KOH and integrating the area under the reduction peak of a stable cyclic voltammogram (CV).

For subsequent studies in KOH, the cycled nickel hydroxide films were again rinsed in deionized (DI) water, heated to the desired temperature at a rate of 5°C per min, maintained at that temperature for 3 h, and subsequently cooled at 5°C per min to room temperature. The oxide films were then cycled in the electrolyte for approximately 25 cycles, and the steady-state capacitances were measured. Prior to conducting an experiment at a different KOH concentration, the films were rinsed in DI water and immersed in the new solution where it was allowed to equilibrate for 15 min. CVs were again performed to measure the capacity once steady state was reached. Studies in H_2SO_4 were conducted by heating the as-deposited film to 300°C as described, but without first cycling in 3 wt % KOH.

A saturated calomel electrode (SCE) and a platinum mesh were used as the reference and counter electrode, respectively, in all experiments. Deposition and cyclic voltammetry studies were conducted on a computer-controlled EG&G Princeton Applied Research M273 potentiostat/galvanostat using the M270 software. The capacity of the films was estimated by integrating the area under the CVs using the software.

Chemically precipitated nickel hydroxide was prepared by adding the nickel nitrate solution described previously into a beaker containing 3 wt % KOH using a dropper. The KOH solution was stirred continuously, thus finely dispersing the precipitated nickel hydroxide. Additional KOH was added to the solution to maintain the pH at 13.0. The resulting nickel hydroxide was filtered using a vacuum arrangement and repeatedly washed in order to remove the KOH from the material. The active material was dried at 80°C for 24 h prior to surface area measurements using the Brunauer-Emmett-Teller (BET) technique. The material was heated to the desired temperature using the same heating regime described and the surface-area measured. The surface-area measurements were performed using a Micromeritics Pulse Chemisorb 2700 analyzer using N_2.

Results and Discussion

Effect of the heating temperature on nickel hydroxide.—Figure 1 shows the CVs of three nickel hydroxide films at a sweep rate of 5 mV/s. The CV of the as-deposited material cycled between −0.80 and 0.55 V *vs.* SCE shows a set of redox peaks corresponding to the nickel oxidation/reduction reaction, often ideally represented as

$$Ni(OH)_2 + OH^- \underset{\text{discharge}}{\overset{\text{charge}}{\rightleftharpoons}} NiOOH + H_2O + e^- \qquad [1]$$
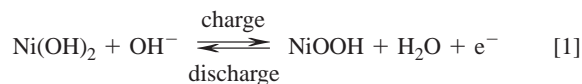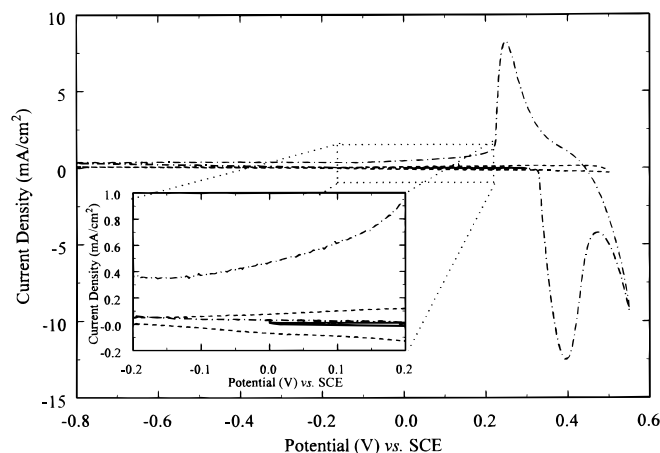
which involves the intercalation/deintercalation of protons. The large anodic currents positive of 0.5 V correspond to the oxygen evo-

* Electrochemical Society Student Member.
** Electrochemical Society Active Member.
z E-mail: weidner@engr.sc.edu

Figure 1. Cyclic voltammetry on: (-·-·-·) an as-deposited film of nickel hydroxide cycled between −0.8 and 0.55 V *vs.* SCE; (- - -) a film heated to 300°C and cycled between −0.8 and 0.50 V; and (—) an as-deposited film cycled between 0.0 and 0.3 V. The sweep rate was 5 mV/s, the electrolyte was 3 wt % KOH, and the cathodic currents are positive.
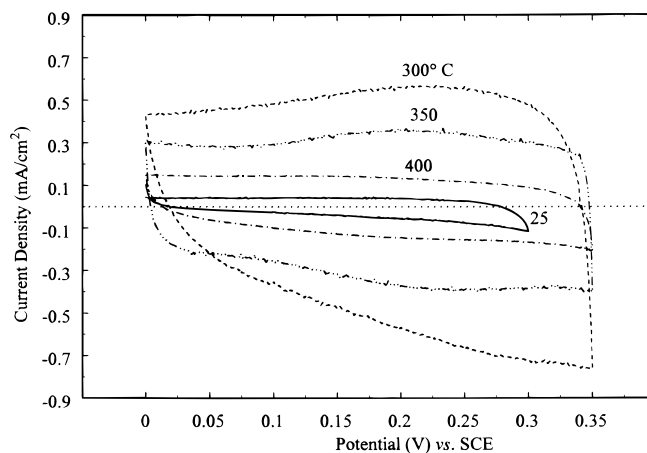

Figure 2. Cyclic voltammetry on nickel hydroxide films that were previously heated to different temperatures. The sweep rate was 20 mV/s, the electrolyte was 3 wt % KOH, and the cathodic currents are positive. (···) Zero current.

lution reaction. When the film is heated to 300°C, the capacity decreases significantly and the current-potential response changes from battery behavior to capacitor behavior. That is, the peaks are no longer visible, and the anodic and cathodic current-potential responses are symmetric about the zero-current axis. This latter point is seen more clearly in the inset to Fig. 1. The response of the as-deposited material cycled between −0.80 and 0.55 V is not symmetric about this axis, even in the potential window between −0.20 to 0.20 V. However, if the as-deposited material is cycled between 0.0 and 0.30 V, below the potential where the oxidation of Ni(OH)$_2$ occurs, the current-potential responses are symmetric about the zero-current axis. Therefore, the as-deposited material behaves as a capacitor as long as Reaction 1 is avoided.

In order to quantify the capacitance of the active material as a function of temperature, CVs were performed in a potential window where Reaction 1 was avoided. For materials heated to 275°C or less, the films were cycled between 0 and 0.3 V, and for materials heated to 300°C and above, the films were cycled between 0.0 and 0.35 V. Four of these steady-state CVs are shown in Fig. 2 in order to confirm that the capacitor behavior is achieved for materials heated between 25 and 400°C. Although the current-potential response is relatively symmetric about the zero-current axis, the capacitance of each film is potential dependent. For example, in the material heated to 300°C, the current, and hence the capacitance, at 0.30 V is twice that at 0.10 V. An ideal capacitor, on the other hand, would exhibit a potential-independent current (*i.e.*, capacitance). Also evident from Fig. 2 is that the capacitance increases when the material is heated from 25 to 300°C but decreases when heated above 300°C. Therefore, Fig. 2 indicates that there is an optimal heating temperature. However, plotting the capacitance rather than the specific capacitance *vs.* temperature may be misleading, since the mass of the film is also changing with temperature. Therefore, the change in structure, and hence the mass, of the active material upon heating is discussed so that the specific capacitance can be estimated.

The electrochemically deposited nickel hydroxide films are very defective, with 25% of the nickel lattice sites containing protons rather than nickel ions.[15,16] This material can be represented stoichiometrically as[17]

$$Ni(2H)_{0.33}O_{2.67}H_{2.67} \cdot X_wH_2O \equiv Ni(OH)_2 \cdot \frac{2}{3}H_2O \cdot X_wH_2O \quad [2]$$
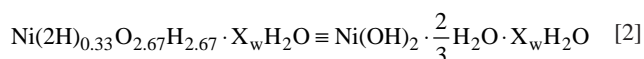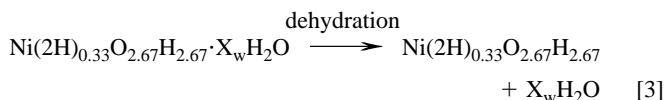
where X_w is the moles of water. This water can be structurally bound to the crystal[18] or in the film between the crystallites. In contrast, the H$_2$O in the "2/3 H$_2$O" is not molecular water but rather two protons sitting on a nickel vacancy with an oxygen atom associated with it.[17]

The redox behavior of this material is well studied as it is the positive electrode in nickel-based batteries and is represented in Reaction 1. Previous studies on heating this material have indicated a three-step weight-loss mechanism based on thermogravimetric analysis (TGA) and differential scanning calorimeter (DSC) results.[18,19] The first two occur when nickel hydroxide is heated to at least 200°C. At this temperature, molecular water is lost from the active material according to the following reaction

$$Ni(2H)_{0.33}O_{2.67}H_{2.67} \cdot X_wH_2O \xrightarrow{\text{dehydration}} Ni(2H)_{0.33}O_{2.67}H_{2.67}$$
$$+ X_wH_2O \quad [3]$$

As shown previously, the dehydrated materials retained the electrochemical signatures of the as-deposited material.[12] Studies on the defect nature of nickel hydroxide have shown that the water content of these films (X_w) is approximately 1 mol of water per mole Ni,[20] which corresponds to a 16% loss in mass via Reaction 3. Therefore, films heated to 200°C have 84% of the mass of the as-deposited material. Note that as X_w contains both structural water and the water between crystallites, one would realistically expect two weight losses, one at ~100°C and the other at ~200°C as observed by previous researchers.[18,19] However, due to difficulty in separating the two phenomenon, it is assumed that a single weight loss occurs at 200°C.

When the film is heated to ~300°C or above, the hydroxide is converted to the oxide[18,19] according to the reaction

$$Ni(2H)_{0.33}O_{2.67}H_{2.67} \rightarrow NiO + 1.67H_2O \quad [4]$$

and the film becomes stoichiometric NiO. The conversion at ~300°C has been shown previously to lead to a significant improvement in the cycle life[12,19] of these materials and a decrease in the optical response.[19] The assumption that the material at 300°C is stoichiometric NiO is reasonable considering the rapid decrease in the level of defects in NiO even at modest heat-treatment conditions.[21] Reaction 4 indicates a further loss of 24% of the mass. Therefore, at or above 300°C the mass of the film is 60% of the as-deposited mass.

The specific capacitance of the active material as a function of heating temperature is plotted in Fig. 3. The specific capacitance of the material was estimated from the CVs by integrating the area under the current-potential curve and then dividing by the sweep rate, the mass of the film, and the potential window according to the equation

$$C = \frac{1}{m\nu(V_a - V_c)} \int_{V_a}^{V_c} I(V)dV \quad [5]$$

For reasons discussed previously, films heated to 200°C were taken to have the mass of the as-deposited material. Films heated above
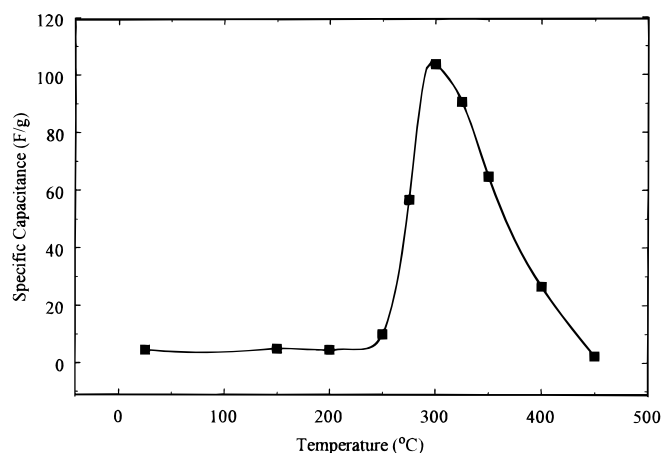
Figure 3. Specific capacitance of nickel hydroxide films that were previously heated to different temperatures. The capacitances were measured using CVs, four of which are shown in Fig. 2. (—) A curve fit through the data points.

Figure 4. Specific surface area and intrinsic capacitance of nickel hydroxide that was previously heated to different temperatures. The surface area was measured from chemically precipitated material using BET. The lines are a curve fit through the data points.

200 but less than 300°C were taken to have 84% of the mass of the as-deposited material, and films heated at or above 300°C were taken to have 60% of the mass of the as-deposited material.

Although an as-deposited nickel hydroxide film exhibits a capacitor-like response when cycled between 0 and 0.30 V *vs*. SCE (see Fig. 2), it does not have a significant specific capacitance (4.7 F/g). As the material is heated, the specific capacitance remains fairly constant until the temperature reaches 300°C. At this temperature, the specific capacitance increases 22 times, to 104 F/g. This dramatic increase in capacitance at 300°C corresponds to the conversion of the hydroxide to the oxide according to Reaction 4. As the film is heated further, the specific capacitance of the oxide reduces until at 450°C the electrode does not store any useful capacity.

The significant change in the specific capacitance on heating can be caused by either (*i*) the formation of a high-surface-area material at ~300°C or (*ii*) pseudocapacitance due to oxide formation. In order to ascertain the cause of the dramatic increase in capacitance at 300°C, BET studies were conducted on bulk precipitated hydroxides at 150, 200, 275, 300, 350, and 400°C. The precipitation was conducted chemically as opposed to electrochemically since it is difficult to deposit electrochemically the requisite quantity of material needed for BET analysis. This is not to argue that the chemical and electrochemical methods yield identical materials, but rather to determine qualitatively how the surface area depends on the heating temperature.

The resulting surface area and intrinsic capacitance (*i.e.*, specific capacitance divided by the surface area) are shown in Fig. 4. The results show that heating the material from 150 to 200°C has a negligible effect on the surface area and intrinsic capacitance of the material. The intrinsic capacitance at these two heating temperatures was estimated to be 4.0 μF/cm², a value consistent with charge storage across a double layer.[4] As the material is heated from 200 to 300°C, a 12% increase in surface area is observed, but the intrinsic capacitance increases by a factor of 17, to 68 μF/cm². Further heating from 300 to 400°C causes the surface area to decrease from 153 to 86 m²/g (a 44% decrease) and the intrinsic capacitance to decrease from 68 to 31 μF/cm² (a 57% decrease).

The effect of the heating temperature on the surface area and the intrinsic capacitance suggests that the dramatic capacitance change at 300°C is due to the formation of NiO. Since the intrinsic capacitance of the NiO is too large to be explained by energy stored across the double layer, its capacitance must arise from the Ni^{2+} to Ni^{3+} redox reaction given by
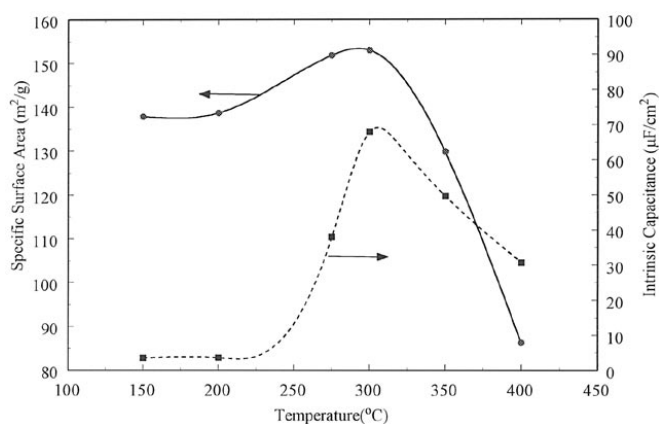
$$NiO + zOH^- \underset{discharge}{\overset{charge}{\rightleftharpoons}} zNiOOH + (1-z)NiO + ze^- \quad [6]$$

Reaction 6 suggests that only a fraction of the nickel sites, *z*, are involved in the redox reaction (*i.e.*, when *z* equals 1.0 all the nickel sites have been oxidized/reduced reversibly).

The value of *z* can be estimated from the specific capacitance of the oxide film by the following relationship

$$z = \frac{CM\Delta V}{F} \quad [7]$$

Using Eq. 7, a potential window of 0.30 V, a molecular weight of 74.7 g/mol, and the specific capacitance from Fig. 3 gives a *z* value of 0.024 and 0.0062 at 300 and 400°C, respectively. In other words, at these respective temperatures only 2.5 and 0.62% of the nickel atoms participate in the reaction that produces the currents in Fig. 2.

These low values of *z* suggest that Reaction 6 is occurring only at the surface of NiO, with little bulk interaction. Unlike nickel hydroxide, where H^+ intercalation into the active material is the mechanism of charge storage, the mechanism in the oxide seems to involve adsorption and reaction of OH^- ions at the surface. Considering the difference in size of H^+ and OH^-, it is not surprising that there is little bulk interaction due to the diffusion of OH^- ions into the material. This is consistent with studies on cobalt oxide[23] and anodically deposited NiO,[22] which concluded that these materials involve predominately surface redox sites. In contrast, a study conducted on hydrous ruthenium oxide[6] has concluded that this material exhibits significant bulk interactions, with a *z* value of approximately 0.85.

If, however, the decrease in specific capacitance above 300°C is only a BET surface-area phenomena, then the intrinsic capacitance shown in Fig. 4 would level off. Since this quantity is also decreasing, the fraction of surface sites participating in Reaction 6 must also be decreasing. In order to quantify this effect, the fraction of nickel atoms that reside on the surface of the active material, ξ, can be calculated from the following formula[23]

$$\xi = \frac{sM}{h^2 L_A} \quad [8]$$

For NiO, the length of the crystal lattice, *h*, is 4.137 Å.[24] At 300 and 400°C, *s* = 153 and 86 m²/g (see Fig. 4) resulting in ξ = 0.11 and 0.062, respectively. Therefore, at 300 and 400°C, only 11 and 6.2% of the nickel atoms, respectively, are at the surface, and of those only 23 and 10%, respectively, are accessed during the CVs shown in Fig. 2 (*i.e.*, *z*/ξ = 0.23 and 0.10, respectively). That the decrease is the percentage of surface sites accessed with temperature means that the electrochemically active surface area decreases at a greater rate than the BET surface area. This is probably due to the isolation of micropores that are no longer accessible to the electrolyte.

The optimum heating temperature of 300°C seen in Fig. 3 occurs when all the hydroxide is converted to oxide but before the electro-

chemically active surface area can be reduced due to sintering of the oxide particles. This optimum is independent of the subsequent cycling conditions (*e.g.*, KOH concentration, potential window) since the predominant changes in microstructure occur during the heating process itself. The heating environment or heating rate, however, could influence the measured capacitance of the material by affecting the surface area or the extent of conversion of the hydroxide to the oxide. Liu and Anderson studied the capacitance of sol-gel-derived NiO films heated in different atmospheres[8] and concluded that air-fired samples show only a slightly higher capacitance compared to heating in pure nitrogen or oxygen. We performed selected experiments at a heating rate of 15°C/min, and no measurable difference in the capacitances or surface areas was detected. In addition, incomplete conversion of the hydroxide to the oxide is easy to detect by the presence of redox peaks in the CV due to Reaction 1. No such peaks were observed at heating temperatures of 300°C and above, indicating complete oxide conversion.

Effect of the electrolyte concentration on the capacitance.—The speculation that the charge-storage mechanism of the nickel-oxide film is due to redox Reaction 6 indicates that significant capacitance should exist only in basic electrolytes. To confirm this hypothesis, experiments were conducted in sulfuric acid and the results compared to those conducted in potassium hydroxide. Figure 5 shows the CVs of two nickel hydroxide films heated to 300°C, one cycled in 3 wt % KOH and the other in 1 N H_2SO_4. The graph clearly indicates the enhanced charge-storage mechanism in basic electrolytes. The capacitance of the material cycled in sulfuric acid (16 F/g) was estimated to be one-sixth the value of the one cycled in KOH (155 F/g). Based on the surface area at 300°C (*i.e.*, 153 m^2/g), an intrinsic capacitance of 10.5 μF/cm^2 is obtained in sulfuric acid, a value consistent with double-layer capacitance.[4] Although previous studies on cycling single crystals of NiO in H_2SO_4 have been reported to exhibit redox peaks due to the oxidation of Ni^{2+} to Ni^{3+} and Ni^{4+},[25,26] no such peaks are evident in Fig. 5. On longer cycles (~50 cycles), a redox peak grows in the CV shown in Fig. 5, consistent with the results of Tench and Yeager.[26] Note that the as-deposited film rapidly dissolves in sulfuric acid, while the film heated to 300°C has no apparent degradation, consistent with the results of Yohe *et al.*[25]

Reaction 6 also suggests that the charge-storage capacity of the film would increase with an increase in the concentration of OH^- ions in solution. To test this hypothesis, CVs from −0.05 to 0.2 V *vs.* SCE were recorded over a wide range of KOH concentrations ranging from 0.5 wt % (0.09 M) to 40 wt % (7.1 M) KOH. The limit of
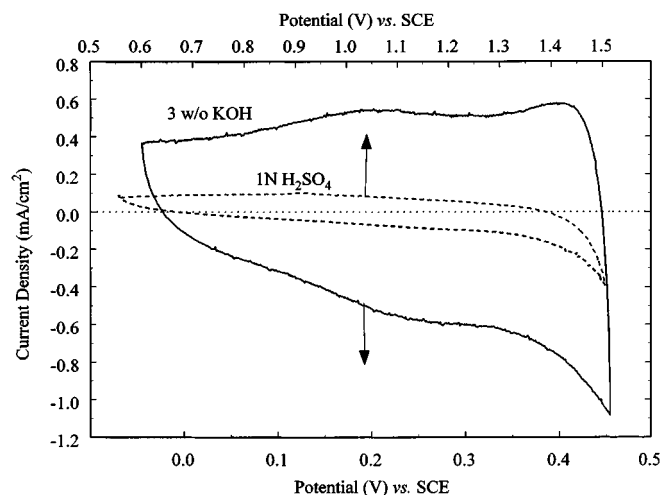
0.2 V was chosen based on the fact that the oxygen evolution reaction according to

$$4\ OH^- \rightarrow O_2 + 2H_2O + 4e^- \qquad [9]$$
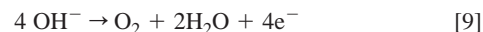
occurs at ~0.25 V in 40 wt % KOH (see Fig. 8). Note that there is a 50 mV decrease in the equilibrium potential of the oxygen evolution reaction when the KOH concentration increases from 0.5 to 40 wt %, as predicted using the Nernst equation for Reaction 9.

Figure 6 shows the specific capacitance as a function of the KOH concentration calculated from the CVs in conjunction with Eq. 5. In Fig. 6, the open circles represent the first set of experiments, where the capacity of the film was estimated at successively increasing concentrations from 0.5 to 40 wt % KOH. The triangles represent the data when the concentration was successively decreased from 40 to 0.5 wt % KOH on the same film. The data points shown in the figure are an average of four experiments on four different films. A clear hysteresis is observed between the two sets of data, indicating that some irreversible changes occurred in the film as the concentration was increased. However, subsequent experiments, involving both increasing and decreasing the concentration on the same film, resulted in capacities within 5% of that obtained in the second data set (*i.e.*, triangles in Fig. 6). Therefore, the second data set also represents the reversible capacity *vs.* concentration data. Note that the capacitance at 3 wt % KOH (*i.e*, 0.54 M) reported in Fig. 6 is lower than the 300°C data reported in Fig. 3 due to the potential-dependent capacitance of the material. The smaller potential window used to generate the data in Fig. 6 results in a small capacitance.

From Reaction 6, one can formulate a rate expression of the form[27]

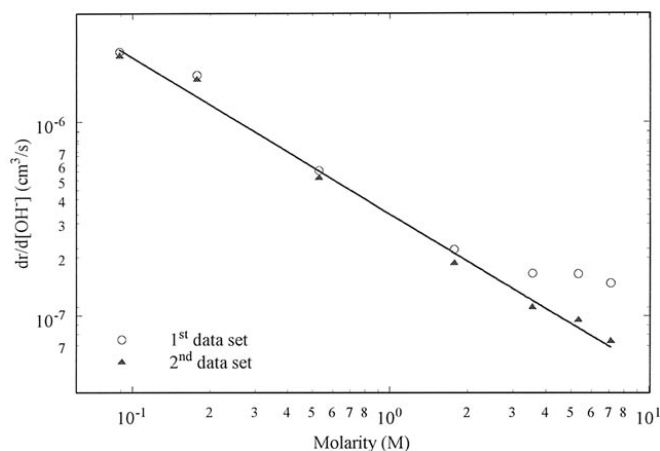$$r = k_f[NiO]^a[OH^-]^b - k_b[NiOOH]^c \qquad [10]$$

Assuming that the number of available nickel sites is independent of the OH^- concentration, differentiating the rate with respect to $[OH^-]$ yields

$$\frac{dr}{d[OH^-]} = k_f b[NiO]^a[OH^-]^{b-1} \qquad [11]$$

Since the specific capacitance data in Fig. 7 were obtained over a fixed time interval (*i.e.*, potential window divided by the sweep rate), they are related to the rate of reaction by the expression
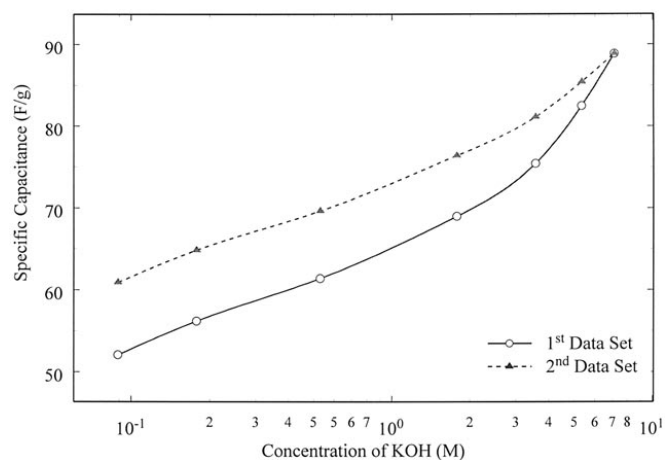
Figure 6. Specific capacitance of nickel oxide films as a function of KOH concentration. The oxide films were formed by heating nickel hydroxide to 300°C. The data points are an average of four experiments on four different films. The first data set is the specific capacitance on films when the concentration was increased consecutively from 0.5 to 40 wt % KOH (*i.e.*, 0.09-7.1 M KOH). The second data set is the specific capacitance when the concentration was decreased from 40 to 0.5 wt % KOH on the same film. Subsequent experiments, involving both increasing and decreasing the concentration on the same film, resulted in capacities within 5% of that represented by the triangles. The lines are a curve fit through the data points.

Figure 5. Cyclic voltammetry on nickel oxide films in: (—) 3 wt % KOH and (- - - -) 1 N H_2SO_4. The oxide films were formed by heating nickel hydroxide to 300°C. The sweep rate was 5 mV/s, and the cathodic currents are positive. (···) Zero current.

Figure 7. The derivative in the nickel redox reaction rate with respect to the KOH concentration as a function of KOH concentration. The rate data were derived by combining the capacitance data in Fig. 6 with Eq. 12. The derivative was calculated at each KOH concentration using finite differences. The data points are an average of four data sets. The line is the best fit of Eq. 11 through the second data set. The slope of the line gives $b = 0.2$.

$$r = \frac{Cvm}{F} \qquad [12]$$

with the assumption that one electron is transferred for every mole of nickel reacted. Therefore, the specific capacitance in Fig. 6 is converted to rate using Eq. 12, and the slope, $dr/d[OH^-]$, is calculated at each KOH concentration using finite differences.[28] A plot of the logarithm of $dr/d[OH^-]$ *vs.* the logarithm of the KOH concentration is shown in Fig. 7. The circles and triangles correspond to the first and second data sets shown in Fig. 6. The line is the best fit through the triangular data points. The slope of the line is (b-1), which gives the reaction order with respect to the OH^- concentration of 0.2. The intercept is related to the rate constant of the forward reaction, the order with respect to the NiO sites, the number of sites, and the order with respect to OH^-.

The best fit of Eq. 11 through the data is the same for both data sets as long as the three highest concentrations for the first data are ignored. The straight line through the data in Fig. 7 suggests that the total number of Ni sites available for reaction is independent of the OH^- concentration. It is possible that at high KOH concentrations the number of Ni sites increases for the first data set, which results in the deviation of the points from the straight line. Such an increase in the number of Ni sites could result from an increase in the surface area of the film at high KOH concentrations, a change that can be expected to be irreversible. However, this irreversible change in structure has no effect on the order of the reaction, which is evident from the relatively constant slope between the two experiments. Once the material has been cycled in high KOH concentrations, the capacitance *vs.* concentration appears to be reversible and follows a straight line represented by the triangles.

Effect of the potential window on electrode operation.—The fact that only 23% of the surface sites are used when the material is heated to 300°C and cycled in 3 wt % KOH is due in part to the limited potential window used. If the anodic limit of the potential window is increased from 0.30 to 0.45 V, the specific capacitance increases from 103 to 132 F/g. This translates into an increase in the percentage of surface sites accesses from 23 to 30%. If the anodic limit of the potential window is decreased to 0.20 V, the specific capacitance decreases to 62 F/g (see triangle at 0.54 M KOH in Fig. 6), and only 14% of the surface sites are accessed. Therefore, increasing the anodic potential limit, holding the electrolyte concentration constant, increases the capacitance.

In addition, the data in Fig. 6 indicates that increasing the KOH concentration, holding the anodic potential limit constant, increases

the capacitance. In practice, however, these two variables are coupled. Lower KOH concentrations result in an increase in the anodic potential limit of the electrode, since oxygen evolution occurs at more positive potentials. This increase would enhance the energy-storage capability of the positive electrode, since the capacitance increases with potential and the energy of a capacitor scales as the square of the potential. In order to demonstrate how the KOH concentration and potential window are coupled, CVs were generated with a fixed cathodic limit of -0.55 V but with an anodic limit adjusted to limit the oxygen evolution current at ~ 1 mA/cm^2. Figure 8 shows the CVs at three different concentrations on a film heated to 300°C. By placing a limit on the amount of oxygen generated, an increase in the KOH concentration results in a decrease in the anodic potential limit and a resulting decrease in the specific capacitance. For example, using only the most positive 0.30 V in Fig. 8, a specific capacitance of 142 F/g is obtained in 3 wt % KOH compared to 130 F/g in 40 wt % KOH. The lower KOH concentrations enable us to access the higher capacitances that are seen at higher potentials. Figure 8 also demonstrates that NiO is best suited as a positive electrode. For example, in 3 wt % KOH the capacitance of NiO is five times larger in the potential window 0.0 to 0.45 V *vs.* SCE compared to the potential window -0.5 to 0.0 V *vs.* SCE.

The effect of the KOH concentration on the overall potential window of the device depends on the choice of the negative electrode, and subsequently, the sensitivity of hydrogen evolution kinetics to KOH concentration. Another factor that must be considered when determining the optimum KOH concentration for a device is the power density. Higher KOH concentrations have greater conductivity (the conductivity of KOH is a maximum at 33 wt %) and hence lead to higher power densities.

Conclusion

Nickel oxide films were fabricated by electrochemically precipitating the hydroxide and heating it to form the oxide. While nickel hydroxide cycled to 0.45 V *vs.* SCE behaves as a battery material due to the proton intercalation reaction, the hydroxide cycled to 0.30 V or the oxide cycled to 0.45 V behaves as a capacitor. The specific capacitance (capacitance per unit mass) of the films was measured as a function of the heating temperature in 3 wt % KOH and over a potential window where no proton intercalation occurs. A negligible increase in specific capacitance was observed as the heating temperature was increased from 25 to 200°C. However, when the heating temperature was increased to 300°C, the specific capacitance increased by a factor of 22.

The large rise in capacitance at 300°C corresponds to the temperature at which the hydroxide is converted to the oxide. Heating to
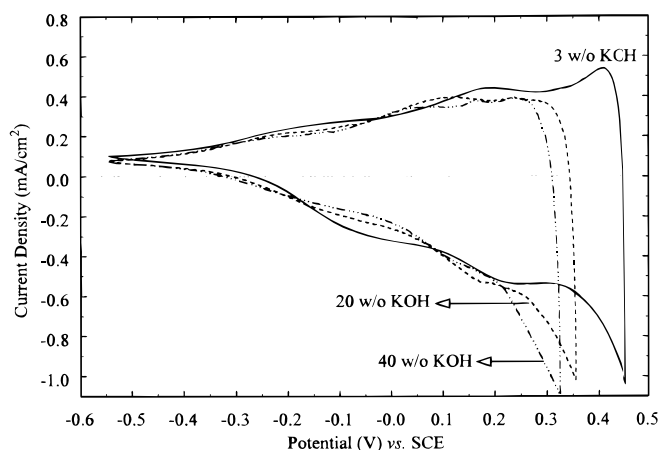
Figure 8. Cyclic voltammetry on a nickel oxide film in different KOH concentrations. The oxide film was formed by heating nickel hydroxide to 300°C. The voltammograms were reversed at the anodic potential limit when the current reached ~ 1 mA/cm^2. The sweep rate was 20 mV/s. ($\cdots$) Zero current.

temperatures above 300°C results in a decrease in the BET surface area and a decrease in the intrinsic capacitance (capacitance per unit BET surface area) of the nickel oxide. Since the intrinsic capacitance decreases with heating temperature, electrochemically active surface area is decreasing faster than the BET surface area. This is probably due to the isolation of micropores that are no longer accessible to the electrolyte.

The large intrinsic capacitance for the oxide suggests that the charge storage is due to a surface redox reaction (*i.e.*, pseudocapacitance), probably involving the adsorption of hydroxyls rather than from a double layer. This was confirmed by cycling the material in different electrolyte environments. In 1 N H_2SO_4, pseudocapacitance was not observed. In KOH, the pseudocapacitance increased with concentration with an estimated reaction order of 0.2, while holding the potential window constant.

Finally, the capacitance of nickel oxide was found to be a strong function of the potential window of operation. Its capacitance was five times larger in the potential window 0.0 to 0.45 V *vs.* SCE compared to the potential window −0.5 to 0.0 V *vs.* SCE, thus making the material best suited as a positive electrode in devices. The potential-dependent capacitance also resulted in a capacitance that decreased with KOH concentration when a fixed oxygen evolution rate was used to determine the anodic potential limit rather than a fixed potential.

Acknowledgments

List of Symbols

a	order of reaction with respect to NiO
b	order of reaction with respect to KOH
c	order of reaction with respect to NiOOH
C	specific capacitance, F/g
F	Faraday constant, 96,487 C/equiv
h	length of crystal lattice, cm
I	current, A
k_b	reverse reaction rate constant for Reaction 6, cm s^{-1} (mol/cm^3)$^{1-c}$
k_f	forward reaction rate constant for Reaction 6, cm s^{-1} (mol/cm^3)$^{1-a-b}$
L_A	Avogadro number, 6.023×10^{23} mol^{-1}
m	mass of the film, g
M	molecular weight, g/mol
r	rate of reaction, mol/cm^3 s
s	specific surface area, cm^2/g
V	potential, V
V_a	anodic potential limit in a CV, V
V_c	cathodic potential limit in a CV, V
z	fraction of nickel atoms involved in the redox process
ΔV	potential window, V

Greek

ν	sweep rate, V/s
ξ	fraction of nickel atoms on the surface

References

1. B. E. Conway, *J. Electrochem. Soc.,* **138,** 1539 (1991).
2. S. Trassati and P. Kurzweil, *Platinum Met. Rev.,* **38,** 46 (1994).
3. S. Sarangapani, B. V. Tilak, and C-P. Chen, *J. Electrochem. Soc.,* **143,** 3791 (1996).
4. A. J. Bard and L. R. Faulkner, *Electrochemical Methods: Fundamentals and Applications,* John Wiley & Sons, Inc., New York (1980).
5. S. T. Mayer, R. W. Pekela, and J. L. Kaschmitter, *J. Electrochem. Soc.,* **140,** 446 (1993).
6. J. P. Zheng, P. J. Cygan, and T. R. Jow, *J. Electrochem. Soc.,* **142,** 2699 (1995).
7. B. E. Conway, in *Electrochemical Capacitors,* F. M. Delnick and M. Tomkiewicz, Editors, PV 95-29, p. 15, The Electrochemical Society Proceedings Series, Pennington, NJ (1995).
8. K.-C. Liu and M. A. Anderson, in *Electrochemical Capacitors,* F. M. Delnick and M. Tomkiewicz, Editors, PV 95-29, p. 68, The Electrochemical Society Proceedings Series, Pennington, NJ (1995).
9. K.-C. Liu and M. A. Anderson, *J. Electrochem. Soc.,* **143,** 124 (1996).
10. K.-C. Liu and M. A. Anderson, in *Electrochemical Capacitors II,* F. M. Delnick, D. Ingersoll, X. Andrieu, and K. Naoi, Editors, PV 96-25, p. 97, The Electrochemical Society Proceedings Series, Pennington, NJ (1996).
11. K.-C. Liu and M. A. Anderson, in *Electrochemical Capacitors II,* F. M. Delnick, D. Ingersoll, X. Andrieu, and K. Naoi, Editors, PV 96-25, p. 85, The Electrochemical Society Proceedings Series, Pennington, NJ (1996).
12. V. Srinivasan and J. W. Weidner, *J. Electrochem. Soc.,* **144,** L210 (1997).
13. C. C. Streinz, A. P. Hartman, S. Motupally, and J. W. Weidner, *J. Electrochem. Soc.,* **142,** 1084 (1995).
14. C. C. Streinz, S. Motupally, and J. W. Weidner, *J. Electrochem. Soc.,* **143,** 4051 (1995).
15. P. L. Loyselle, P. J. Karjala, and B. C. Cornilsen, in *Electrochemical and Thermal Modeling of Battery, Fuel Cell and Photoenergy Conversion Systems*, R. J. Selman and H. C. Maru, Editors, PV 86-12, p. 114, The Electrochemical Society Proceedings Series, Pennington, NJ (1986).
16. B. Cornilsen, X. Cai, R. Tanbug, and G. Meitzner, in *Aqueous Batteries,* P. D. Bennett and S. Gross, Editors, PV 96-16, p. 88, The Electrochemical Society Proceedings Series, Pennington, NJ (1997).
17. Z. Xu, B. C. Cornilsen, and G. Meitzner, in *Selected Battery Topics,* G. Halpert, M. L. Gopikanth, K. M. Abraham, W. R. Cieslak, and W. A. Adams, Editors, PV 98-15, p. 1, The Electrochemical Society Proceedings Series, Pennington, NJ (1999).
18. M. Mani and J. P. de-Neufville, *J. Electrochem. Soc.,* **135,** 800 (1988).
19. C. Natarajan, H. Motsumoto, and G. Nagomi, *J. Electrochem. Soc.,* **144,** 121 (1997).
20. V. Srinivasan, B. C. Cornilsen, and J. W. Weidner, in *Selected Battery Topics,* G. Halpert, M. L. Gopikanth, K. M. Abraham, W. R. Cieslak, and W. A. Adams, Editors, PV 98-15, p. 31, The Electrochemical Society Proceedings Series, Pennington, NJ (1999).
21. D. A. Wruck and M. Rubin, *J. Electrochem. Soc.,* **140,** 1097 (1993).
22. S. Cordoba-Torresi, A. Hugot-Le Goff, and S. Joiret, *J. Electrochem. Soc.,* **138,** 1554 (1991).
23. C. Lin, J. A. Ritter, and B. N. Popov, *J. Electrochem. Soc.,* **145,** 4097 (1998).
24. *CRC Handbook of Chemistry and Physics,* CRC Press, Inc., Boca Raton, FL (1979).
25. D. Yohe, A. Riga, R. Greef, and E. Yeager, *Electrochim. Acta,* **13,** 1351 (1968).
26. D. M. Tench and E. Yeager, *J. Electrochem. Soc.,* **120,** 164 (1973).
27. O. Levenspiel, *Chemical Reaction Engineering,* John Wiley & Sons, Inc., New York (1972).
28. S. C. Chapra and R. P. Canale, *Numerical Methods for Engineers,* 2nd ed., McGraw-Hill, Inc., New York (1988).